HHS Public Access

Author manuscript

Gene Ther. Author manuscript; available in PMC 2015 September 01.

Published in final edited form as:

Gene Ther. 2015 March ; 22(3): 257–266. doi:10.1038/gt.2014.97.

Phospholipid-modified PEI-based nanocarriers for *in vivo* siRNA therapeutics against multi-drug resistant tumors

Sean Essex[#], **Gemma Navarro**[#], **Pooja Sabhachandani**, **Aabha Chordia**, **Malav Trivedi**, **Sara Movassaghian**, and **Vladimir P. Torchilin**[**]

Center for Pharmaceutical Biotechnology and Nanomedicine, Northeastern University, Boston, MA 02115, USA

[#] These authors contributed equally to this work.

Abstract

Multidrug resistance (MDR) mediated by P-glycoprotein overexpression in solid tumors is a major factor in the failure of many forms of chemotherapy. Here, we evaluated phospholipid-modified, low molecular weight polyethylenimine (DOPE-PEI) nanocarriers for intravenous delivery of anti-P-pg siRNA to tumors with the final goal of modulating MDR in breast cancer. First, we studied the biodistribution of DOPE-PEI nanocarriers and the effect of PEG coating in a s.c. breast tumor model. Four hours post-injection, PEGylated carriers showed an 8% injected dose (ID) accumulation in solid tumor via the enhanced permeability and retention effect and 22% ID in serum due to a prolonged, PEG-mediated circulation. Second, we established the therapeutic efficacy and safety of DOPE-PEI/siRNA-mediated P-gp down-regulation in combination with Doxorubicin (Dox) chemotherapy in MCF-7/MDR xenografts. Weekly injection of siRNA nanopreparations and Dox for up to 5 weeks sensitized the tumors to otherwise non-effective doses of Dox and decreased the tumor volume by 3-fold versus controls. This therapeutic improvement in response to Dox was attributed to the significant, sequence-specific P-gp down-regulation in excised tumors mediated by the DOPE-PEI formulations.

Keywords

Small interfering RNA (siRNA); Polyethylenimine (PEI); Phospholipid conjugation; Polyethyleneglycol (PEG); Breast cancer; Multidrug resistance (MDR); P-glycoprotein (P-gp); Doxorubicin (Dox)

INTRODUCTION

Resistance to chemotherapy is a serious challenge for the effective treatment of breast cancer. The development of multidrug resistance (MDR), mediated by the overexpression of the adenosine triphosphate (ATP) binding cassette (ABC-transporters) is believed to play an

[**]Corresponding author: Center for Pharmaceutical Biotechnology and Nanomedicine, Northeastern University, 360 Huntington Ave, 140 The Fenway, Room 211/214. Boston, MA 02115, USA. Tel.: +1 617 373 3206. v.torchilin@neu.edu.

CONFLICT OF INTEREST The authors declare no conflict of interest.

important role in the poor efficacy of cancer chemotherapy [1, 2]. P-glycoprotein (P-gp), a 170-kDa plasma membrane glycoprotein, was the first ABC transporter consistently identified to be overexpressed in breast cancer cell lines displaying MDR. It employs ATP to actively pump cytotoxic drugs out of the cells and is responsible for the efflux of chemotherapeutic drugs such as vinblastine, doxorubicin, and paclitaxel which leads to a decreased accumulation of drug in tumor cells and consequently, the failure of chemotherapy [3]. To circumvent MDR, P-gp represents an attractive target that is over-expressed at up to 30% in newly diagnosed cancers and over 70% in relapsed forms of breast cancer [4].

P-gp-mediated MDR can be reversed using small molecules acting as P-gp substrates or inhibitors. However, their clinical use is associated with intolerable side-effects and toxicity due to off-target distribution and pharmacokinetic interactions with anticancer drugs [5-11]. An alternative approach to inhibition of P-gp activity is to down-regulate its expression at the transcriptional level by using short double-stranded RNAs, so-called siRNA, that trigger the catalytic degradation of complementary mRNAs [12-14]. Clear advantages of the siRNA approach compared to chemical inhibitors include its reduced toxicity towards non-specific tissues (since siRNA cannot diffuse passively through cellular membranes) and its high specificity. However, the targeted delivery of siRNA into tumor cells following a systemic application is difficult due to its poor *in vivo* stability (rapid degradation in plasma and cellular cytoplasm) and poor cellular uptake [15]. The development of parenteral siRNA formulations that are stable in the circulation, promote tumor accumulation and that lack carrier-related toxicities is essential for the clinical use of siRNA-based drugs. One of the most investigated carriers is polyethylenimine (PEI), which functions as a transfection reagent based on its ability to compact siRNA into nano-scale complexes. This feature offers protection from harsh enzymatic degradation and improves both intracellular delivery of siRNA and trafficking uptake through endocytosis and escape from lysosomes [16, 17]. The transfection efficiency/cytotoxicity profile of PEIs is largely influenced by their molecular weight. With the increase in their molecular weight, branched PEIs exhibit increased transfection that also correlates with increased non-specific toxicity due to excessive interactions with cell membranes by the cationic charges of PEI. Low molecular weight (LMW) PEIs have low toxicity and are hemocompatible but display poor transfection [18-20]. We previously reported that chemical conjugation of DOPE phospholipid to low molecular weight PEI (1.8 kDa) significantly improved the intracellular siRNA delivery and the gene silencing of non-modified PEI while keeping cytotoxicity levels low [21, 22]. The present study reports on the *in vivo* utility of these DOPE-PEI nanocarriers. In particular, we evaluated their tissue distribution upon intravenous injection in tumor-bearing mice and the effect of PEG coating as a strategy to improve their stability in circulation and enhance permeability and retention by the tumor [23-25]. In a second step, we evaluated the anti-cancer activity of DOPE-PEI/anti-P-gp siRNA nanopreparations and Dox combinations in resistant breast cancer MCF-7/ADR xenografts. The scheme of the proposed experiment is depicted in Fig. 1. We used different dosing regimens, i.e. simultaneous vs. sequential administration of siRNA and Dox to optimize their anti-cancer activity. To the best of our knowledge, this is the first study that demonstrates the utility of LMW PEI (1.8 kDa) for i.v. siRNA delivery

to tumors for the reversal of P-gp resistance to Dox and investigates the impact of different delivery modes on the therapeutic outcome of siRNA/drug combinations.

RESULTS

Biophysical characterization of the formulations

DOPE-PEI/siRNA complexes were prepared as described [22]. The complexes were also mixed with the micelle-forming material, 1,2-distearoyl-sn-glycero-3-phosphoethanolamine-N-[methoxy (polyethyleneglycol)-2000] (PEG-PE), to improve stability [26]. The biophysical characterizations of DOPE-PEI/siRNA and DOPE-PEI/PEG/siRNA are shown in Fig. 2. The detailed structure and the effect of PEG addition on the morphology of the formulations was studied by dynamic light scattering (DLS), atomic force microscopy (AFM), and transmission electronic microscopy (TEM). DLS was used to determine the hydrodynamic diameter of the complexes whereas, AFM and TEM were chosen as methods that allowed sample visualization, measurement of the real size (not the hydrodynamic) of the complexes and additionally gave a three dimensional profile of the sample (in the case of AFM). The formation of the PEG-PE corona around the DOPE-PEI/siRNA core was proposed based on the fact that the zeta potential drastically changed from an average of about + 48 mV for DOPE-PEI/siRNA complexes to about + 13 mV after the addition of PEG-PE, suggesting a cationic charge-shielding effect, whereas the mean size measured by DLS was not affected by the addition of PEG (Fig 2A). The zeta potential for free PEG-PE micelles was - 27 ± 8 mV in accordance with reported values [27]. By AFM analysis, the DOPE-PEI/siRNA complexes appeared as well-developed, individualized, rounded particles with a broad size distribution ranging from 50-500 nm. DOPE-PEI/PEG/siRNA particles exhibited an almost spherical shape and a narrower size distribution. TEM analysis of DOPE-PEI/siRNA and DOPE-PEI/PEG/siRNA complexes confirmed the protective and stabilizing effect of the PEG-PE corona. The DOPE-PEI/siRNA complexes appeared like ovoid particles. Some concentric ovoid structures were also visualized with a mean particle size of 110.4 ± 20.4 nm. The DOPE-PEI/PEG/siRNA micelles appeared as almost spherical particles (Fig. 2B). The mean particle size for the DOPE-PEI/PEG/siRNA complex was 95.8 ± 38.7 nm.

We also monitored the stability of the DOPE-PEI/siRNA nanocarriers (PEGylated and non-PEGylated) in 150 mM NaCl. The benefit of PEGylation was clear: the PEGylated nanocarrier exhibited no signs of aggregation in contrast to the non-PEGylated nanocarrier **(**Fig. 2C**)**. Although *in vitro* experiments with highly concentrated formulations (40 μg siRNA per 100 μL of formulation) demonstrated fast aggregation for the non-PEGylated formulation, we proposed that *in vivo*, due to the rapid dilution with the volume of blood, that aggregation would be prevented and physiological activity preserved. This was confirmed in the efficacy study (see further).

Biodistribution study

For biodistribution studies, 4T1 murine breast cancer cells were chosen to induce tumors since this is a well-established animal model closely mimicking human metastatic breast cancer [28], and it is fairly simple to induce these tumors quickly in female Balb/c mice. Figure 3 depicts the biodistribution 4 h post-injection of fluorescently labeled siRNA

loading with different formulations. Our data indicate an enhanced blood circulation for DOPE-PEI/PEG/siRNA complexes when compared to DOPE-PEI/siRNA complexes (22%ID vs 9% ID) and naked siRNA, for which no detectable fluorescence signal was measured. PEGylated formulations had significantly better tumor accumulation as compared to naked siRNA (8% ID vs 4% ID). DOPE-PEI nanocarriers delivered higher siRNA doses in lung and liver as compared to PEGylated formulations (14% ID vs 6% ID and 19% ID vs 13% ID, respectively). Inclusion of PEG-PE in formulations shielded the non-specific interactions with these organs and led to % ID values similar to those of the naked siRNA. The highest fluorescent signal of about 20% ID was detected in kidney where no difference between formulated and non-formulated siRNA accumulation was observed.

Development of MCF7/ADR and MCF7/S orthotopic and subcutaneous tumor models and qRT-PCR characterization

Due to the conflicting literature regarding the development of MCF-7/ADR tumors and the need for β-estradiol supplementation for the growth of MCF7/ADR xenografts [29-33], we decided to first optimize tumorigenic conditions for MCF7/ADR cells in female nude mice. Mice were injected orthotopically in the mammary fat pad or subcutaneously (s.c.) over the right flank with these cells as described in the methods section. The tumors were allowed to develop for five weeks after which the mice were sacrificed and their tumors excised. The tumors sizes in the two orthotopic tumors MCF-7/ADR were similar with or without estrogen supplementation (mean volume approx. 40 mm^3). The qRT-PCR data clearly showed that the MDR1 levels in the MCF7/ADR orthotopic tumors in the presence or absence of the estradiol were very similar suggesting that, in contrast to orthotopic MCF7/S tumors, the growth of MCF7/ADR orthotopic tumors was estrogen-independent. The implantation of the estradiol pellet did not affect tumor volume or MDR1 gene expression five weeks post-tumor inoculation. On the other hand, the subcutaneous (s.c) tumors (about 100 mm^3) had a lower MDR1 level compared to the MCF7/ADR orthotopic tumors, albeit they had significantly higher MDR1 levels than the orthotopic MCF7/S tumors **(**Fig. 4**).** The s.c. model was chosen for the final therapeutic efficacy experiments since larger tumors were obtained in a shorter period of time, and the tumors retained high MDR1 levels.

Therapeutic efficacy study

The therapeutic effect of siRNA targeting P-glycoprotein (siMDR1) formulated in DOPE-PEI nanocarriers (PEGylated and non-PEGylated) in combination with Dox was evaluated in resistant breast MCF-7/ADR tumors (Fig. 5). The mice were randomized for treatment after the s.c. tumor volume reached 60 mm^3. The dosing regimen was one naked siRNA or formulation containing siRNA injection followed by one Dox injection after 48 h (sequential regimen). This dosing regimen was carried on for 5 weeks. Five days after the final dose, the mice were sacrificed. The Dox effect was assessed by monitoring the tumor volume during the treatment and by the final weight of the post-mortem excised tumors. Although, in this study we aimed just to confirm the improved therapeutic outcome by using the suggested preparation rather than to analyze its detailed action mechanism, the P-gp downregulation is clearly be as shown by us and in similar setting by quantifying the levels of P-gp (mRNA and protein) in the experimental tumors as in [34-36].

The combination of DOPE-PEI/ or DOPE-PEI/PEG/siMDR1 and Dox resulted in sensitization of resistant tumors to Dox and improved its anti-cancer activity. Both treatments significantly inhibited the tumor growth relative to all control groups including buffer control, free siMDR1+ Dox and DOPE-PEI/scramble siRNA + Dox ($P < 0.001$). No significant difference was observed between PEGylated and non-PEGylated formulations. The treated mice showed a 3-fold reduction in tumor volume (RTVm) as compare to control groups **(**Fig. 5A**)** that was consistent with the half-reduction in tumor weight measured after the sacrifice of the animals **(**Fig. 5B**)**. DOPE-PEI /scrambled siRNA had no therapeutic advantage, which demonstrates the relevance of the MDR1 siRNA sequence specificity for therapeutic efficacy. Free siMDR1 in combination with Dox did not show any significant difference with respect to the buffer control in terms of tumor inhibition, confirming our previous *in vitro* studies showing that the association of siRNA with DOPE-PEI nanocarriers is essential to deliver and internalize siRNA into tumor cells, mediate P-gp downregulation and restore Dox resistance [22]. To confirm P-gp (MDR1) down-regulation in excised tumors, qRT-PCR was performed for evaluation of the transcriptional mRNA levels of the MDR1 gene **(**Fig. 5C**)**, and flow cytometry was performed to check the P-gp protein level expression on the surface of the tumor cells **(**Fig. 5D**)**. Free siMDR1 and DOPE-PEI / scrambled siRNA did not show any significant differences in P-gp suppression compared to buffer control. However, MDR1 mRNA levels were reduced by half in those tumors treated with DOPE-PEI/siMDR1 and almost completely abrogated after DOPE-PEI/PEG/siMDR1 treatment. Similarly, the overexpression of P-gp protein in resistant tumors was restored to the levels observed in sensitive tumor cells after DOPE-PEI/PEG/ and DOPE-PEI/siMDR1 treatments. The slightly greater P-gp down-regulation found for PEGylated nanopreparations did not correlate with a better response of tumors to Dox.

A second therapeutic experiment was performed to check the effect of the dosing regimen. In particular, we evaluated whether the different administration of the DOPE-PEI/siRNA nanocarrier and Dox, sequential or simultaneous, would have a different effect on P-gp suppression and tumor growth. With this in mind, three groups of female nude mice (n=5) bearing MCF7/ADR tumor xenografts, were treated as follows in a manner similar to the conditions in the previous therapeutic efficacy study: Group 1 – naked therapeutic MDR1 siRNA + Dox administration at +48 h; Group 2 – DOPE-PEI/MDR1 siRNA + Dox administration at +48 h (sequential); Group 3 - DOPE-PEI/MDR1 siRNA followed by immediate Dox injection (simultaneous). At day 20, the sequential administration of the treatments resulted in significantly better tumor inhibition than their simultaneous administration (5-fold and 2-fold tumor volume reduction, respectively, as compared to buffer control). However, at the end of the study (day 40), both regimes turned out to be equally effective with a 3-fold tumor volume reduction as compared to free siRNA + Dox treatment **(**Fig. 6A**).** The anti-cancer activity was associated with significant down-regulation of MDR1 observed in the excised tumor and was higher in the case of the co-administration group (Fig. 6 B and C).

To monitor the overall health of the animals, animal weights were recorded throughout the study. The levels of amino transferases (AST and ALT) in serum were also analyzed as indicator of repeated dosing toxicity in liver [37]. The animals tolerated the treatments well.

No significant loss in body weight or evidence of hepatotoxicity was observed **(**Tables 1 **and** 2**).**

DISCUSSION

Resistance to chemotherapy is a major cause of treatment failure and relapse of many cancer types, including breast cancer. Approaches based on a combination of chemotherapeutics with gene silencing molecules to suppress the expression of efflux transporters, such as P-glycoprotein are currently among the most widely investigated drug-nucleic acid combinations for cancer therapy [22, 36, 38-42]. The translation of such combinations to animal models has been challenging due to an unfavorable siRNA pharmacokinetic profile, low tumor accumulation and a lack of safe and efficient delivery systems.

We recently showed that DOPE-PEI conjugates based on low molecular weight PEI self-assembled within micellar structures that condensed siRNA, had high transfection efficiency and had a better toxicity profile than PEI 25 kDa and Lipofectamine. The DOPE-PEI/anti-P-gp siRNA nanopreparations inhibited P-gp expression and enhanced the intracellular delivery and the cell killing by Dox in resistant breast cancer cells (MCF-7/ADR) [22]. Here, we tested their utility for systemic delivery of anti-P-gp siRNA to tumors in combination with Dox chemotherapy. We incorporated PEG-PE in the carriers to achieve enhanced tumor delivery and to improve their performance upon intravenous injection. We proposed that PEG-PE would spontaneously incorporate into DOPE-PEI due to the hydrophobic interactions and additionally provide some steric stabilization of complexes by forming a protective barrier, shielding the positive charge and promoting increased stability in high-salt conditions. The DOPE-PEI complexes with PEG-PE were stable in 150 mM NaCl with no significant change in size **(**Fig. 2C**)**. Hydrophobic interactions between the lipid moieties in DOPE-PEI and those in PEG-PE resulted in their self-assembly into micelle-like particles **(**Fig. 2B**)**. A similar hydrophobic interaction was suggested between the amphiphilic Pluronic chains of Pluronic -grafted PEI, which form a micelle-like structure around the polyplex core and unmodified Pluronic [43, 44].

A biodistribution study was performed to investigate the *in vivo* behavior (circulation, tissue distribution, absence of acute toxicity) of DOPE-PEI nanocarriers and to test if the effects of PEG inclusion, mainly hindrance of positive charge and improved stability, would be beneficial *in vivo* **(**Fig. 3**)**. The results of biodistribution studies of the different formulations of siRNA at 4h post-injection have clearly confirmed prolonged circulation and good tumor accumulation for DOPE-PEI/PEG/siRNA preparations as compared to naked siRNA for which no fluorescence signal in blood and low tumor accumulation were found, and our numbers are in good agreement with previous reported data[45-47], which showed tumor accumulation from 0.5 to 10% of the injected dose of labelled free siRNA at similar time-point despite its fast degradation and complete elimination from the blood. A decreased interaction with serum proteins, a lower accumulation in the lung and a decreased mononuclear phagocyte system (MPS) uptake allowed the formulation to circulate *in vivo* for a longer time and resulted in greater accumulation in the tumor via the EPR effect [23-25]. Recently, two studies have reported on the biodistribution of PEG-grafted PEI 25k Da/siRNA complexes in healthy mice[47, 48]. Similar to our observations, inclusion of PEG in

PEI 25 kDa/siRNA formulations stabilized siRNA in blood and decreased non-specific interactions with lung and liver by shielding the positive charge of PEI complexes that otherwise can cause acute toxicity (erythrocyte aggregation, pulmonary embolism, hepatotoxicity) [47, 48]. We found high levels of siRNA in the kidney (about 20% ID) regardless of the formulation. This is an expected phenomenon since naked siRNA is rapidly excreted by the kidneys [49]. In the case of complexes, interaction between the negatively charged basal membrane of the Bowman's capsule and the cationic complexes occurs [50].

Once we evaluated the biodistribution of DOPE-PEI nanocarriers and confirmed that the inclusion of PEG improved the biodistribution pattern of siRNA (not only in terms of better tumor delivery but also by decreasing DOPE-PEI/siRNA non-specific interactions with lung and liver), we moved to optimize the MCF-7/ADR animal model to test the therapeutic application of the nanocarriers using P-glycoprotein-siRNA/Dox combinations that previously showed positive results in MCF-7/ADR cell culture [22]. Combination of DOPE-PEI/ or DOPE-PEI/PEG/siMDR1 and Dox resulted in sensitization of MCF-7/ADR resistant tumors to Dox and improved *in vivo* anti-cancer activity. Weekly administration of 2 mg/kg of Dox + Free siMDR1 had no therapeutic effect, whereas the sequential administration of anti-P-gp nanopreparations and Dox mediated specific down-regulation of P-gp in the tumors and inhibited their growth **(**Fig. 5A and B**)**. The elevated P-gp levels that occurred in resistant tumors were lowered to those of MCF-7 sensitive cells **(**Fig. 5D**)**. In the case of DOPE-PEI/PEG/siMDR1, P-gp down-regulation was even more pronounced **(**Fig. 5C and D**)**. Interestingly, the slightly greater P-gp down-regulation found for PEGylated nanopreparations did not produce a greater anti-cancer effect. Both treatments significantly inhibited the tumor growth relative to all control groups, but no significant difference was observed between PEGylated and non-PEGylated formulations. A possible explanation for the absence of differences may be the use of low doses of Dox. The non-PEGylated formulation produced a robust suppression of P-gp. If the maximum Dox anti-cancer effect had already been achieved for this P-gp suppression, incremental P-gp suppression by a PEGylated formulation would not lead to an incremental anti-cancer effect. For this proof-of-concept study, we employed non-effective low doses of Dox (2mg/kg) to show the effectiveness of the addition of siRNA nanopreparations. Future experiments will test higher doses of Dox to help to discriminate different levels of P-gp downregulation and optimize their anti-cancer activity. Jiang and collaborators demonstrated significant inhibition of tumor growth in the same MCF-7/ADR tumor model by using RGD-modified liposomes containing Anti-P-gp siRNA (2 mg/kg) or Dox (4 mg/kg) [36]. Similar to our results, they found a 3-fold decrease in the RTVm compared to buffer controls and a 2-fold decrease in RTVm when compared to liposomal Dox alone. However, systemic toxicity (a 20% loss weight) resulted from Dox treatments. In the case of MCF-7 sensitive tumors, Dox doses in the range of 1.5 to 5 mg/kg produced 50 to 60% tumor inhibition rates [51-53].

The rationale for the sequential administration of anti-P-gp siRNA and chemotherapy is that the inhibition of efflux mechanisms has to precede the chemotherapy treatment for the maximum anti-cancer effect. Therefore, a time lapse (24-48h) between P-gp siRNA and the chemotherapy drug is usually included in the majority of the experimental protocols to allow for sufficient target protein down-regulation. This notion is supported *in vivo* by studies in

MDR tumors [36, 54, 55]. On the other hand, the simultaneous delivery of siRNA and chemotherapy, mostly by the co-loading of the agents in a single carrier, has also been shown to effectively reverse MDR [41, 56, 57]. The rationale behind this approach is that a temporary co-localization of the anti-cancer drug and the siRNA against P-gp in the same cancer cell can promote a better anti-cancer activity. To date, *in vivo* studies that have investigated and compared the effects of multiple injections and different regimens of administration on gene suppression and therapeutic responses mediated by siRNA/drug combinations are rare[58]. There is a great need of a better understanding of the mechanistic and kinetic aspects involved in these anti-cancer combinations. The optimal sequence of administration of siRNA and drug for the maximum anti-cancer responses has not been elucidated yet.

With this in mind, we compared the effect of sequentially or simultaneously administered siRNA nanopreparations and Dox on P-gp down-regulation and anti-tumor activity over a period of 5-weeks treatment **(**Fig. 6**)**. The administration mode had no impact on the final therapeutic outcome. Both regimens turned out to be equally effective in inhibiting tumor growth. This is in agreement with our previous findings performed with MCF-7/ADR cells [22], where the activity of Dox was significantly increased by anti-P-gp siRNA/DOPE-PEI preparations regardless of the time lag (0-48 h) between the treatments. On the other hand, the co-administration of siRNA nanopreparations and Dox showed higher down-regulation of P-gp in the tumors **(**Fig. 6B and C**)**. At low doses, Dox behaves like an anti-angiogenic agent, expanding the interstitial space, vessel diameter and blood perfused area [38]. In the co-administration group, it is possible that the carrier penetration was improved by this phenomenon, especially if the carrier and the drug co-existed spatially. It has been shown that free Dox injected i.v. has a plasma half-life of about 16 ± 3 h in nude tumor-bearing mice, [59] and our biodistribution data prove that DOPE-PEI nanocarriers can deliver siRNA to the tumor within 4 h (5 % ID in tumor and 10% ID in blood, Figure 3).

In conclusion, we demonstrated the usefulness of DOPE-PEI nanocarriers for intravenous delivery of siRNA to tumors. We showed that DOPE-PEI nanocarriers loaded anti-P-gp siRNA can be used to suppress P-gp activity and restore Dox sensitivity in resistant human breast cancer tumors. The nanopreparations had small particle sizes (< 150nm) compatible with parenteral administration and showed improved colloidal stability when PEG was incorporated in the formulation. In addition, PEGylated formulations showed prolonged circulation and improved siRNA tumoral delivery via an EPR effect as compared with non-PEGylated ones. DOPE-PEI based-nanopreparations, regardless of the presence of PEG, deliver sufficiently high amounts of siRNA to mediate specific P-gp down-regulation in resistant tumors and restore their sensitivity to otherwise non-effective doses of Dox. Simultaneous or sequential weekly administration of anti-P-gp siRNA nanopreparations and Dox were equally effective in inhibiting tumor growth over a period of 5-weeks and were well-tolerated by the animals.

MATERIALS & METHODS

Materials

All materials were purchased from Sigma-Aldrich unless otherwise stated. Branched polyethylenimine [60] with a molecular weight of 1.8 kDa was purchased from Polysciences, Inc. (Warrington, PA). 1,2-distearoyl-sn-glycero-3-phosphoethanolamine-N-[methoxy (polyethyleneglycol)-2000] (PEG-PE) and 1,2-dioleoyl-sn-glycero-3-phosphoethanolamine-N-(glutaryl) (Glutaryl-PE) were purchased from Avanti Polar Lipids (Alabaster, AL). All siRNA duplexes were purchased from Dharmacon (Lafayette, CO), namely, Fluorescein labeled siRNA (FL-siRNA), siRNA targeting MDR1 (siMDR1): 5′-GGAAAAGAAACCAACUGUCdTdT-3′ (sense) 61, and a non-targeting control siRNA, (scramble siRNA): 5′-AGUACUGCUUACGAUACGGdTdT-3′(sense). FITC-labeled P-glycoprotein antibody [UIC2] was purchased from Abcam (Cambridge, MA). The CellTiter-Blue® Cell Viability Assay was purchased from Promega (Madison, WI). Nuclease-free water was purchased from Qiagen (MD, USA). The Aspartate aminotransferase (AST)/ Alanine aminotransferase (ALT) assay kit was purchased from the Biomedical Research Service Center at SUNY Buffalo (Buffalo, NY). The RNAeasy kit for mRNA islolation was obtained from Qiagen (MD, USA). The first strand cDNA synthesis kit and the SYBR green kit for qRT-PCR were obtained from Roche (IN, USA). Primers for the dsMDR1 gene (5′-ATATCAGCAGCCCACATCAT-3′) and (5′-GAAGCACTGGGATGTCCGGT-3′) and for the housekeeping gene GAPDH (5′-GCCAAAAGGGTCATCATCTC-3′) and (5′-GTAGAGGCAGGGATGATGTTC-3′) were obtained from Invitrogen (CA, USA).

Cell Culture

The 4T1 mammary carcinoma cells were obtain from the American Type Culture Collection (Manassas, VA) 28. The wild-type (sensitive) and Dox-resistant MCF-7 human breast adenocarcinoma cells were kindly provided by Dr. T. Minko (The State University of New Jersey, NJ, USA). The resistant MCF-7 phenotype has been previously characterized as overexpressing the MDR1 gene [62, 63]. Cell lines were grown at 37°C under 5% CO_2 in DMEM supplemented with 10% fetal bovine serum and penicillin (100 units/ml) and streptomycin (100 μg/ml). DMEM and penicillin/streptomycin stock solutions were purchased from Cellgro (VA, USA). Bovine serum albumin and heat-inactivated fetal bovine serum was purchased from Atlanta Biologicals (GA, USA).

Methods

Sample preparation and characterization—The DOPE-PEI conjugate and the DOPE-PEI/siRNA complexes were prepared as previously described[21, 22]. Briefly, for the preparation of the phospholipid-PEI/siRNA complexes, fixed amounts of siRNA and varying amounts of phospholipid-PEI conjugates were diluted separately in equal volumes (50 μL) of buffered HEPES glucose (HBG, pH 7.4, nuclease-free water). The siRNA solution was transferred to the polymer solution, mixed by smooth pipetting and incubated for 15-20 min at room temperature. A PEGylated formulation viz. DOPE-PEI/PEG/siRNA was prepared by adding a DOPE-PEI/siRNA complex solution prepared in HBG at N/P 16, to a previously freeze dried lipid film of PEG-PE (DOPE-PEI:PEG-PE was 1:10 w/w) and allowed to stand at room temperature for 30 min with intermittent shaking [26].

The formulations were characterized for particle size distribution and zeta potential by Dynamic light scattering (DLS) using a Malvern Zetasizer ZS90 Nano instrument (Malvern Instruments, Westborough, MA). Briefly, 100μl of freshly prepared formulation was diluted suitably in nuclease free water and the size and zeta measurements were obtained. The morphological properties of the nanopreparations were also evaluated using Atomic Force Microscopy (AFM) and Transmission Electron Microscopy (TEM).

Atomic Force Microscopy (AFM)—The DOPE-modified PEI nanocarriers were characterized by AFM as a supplementary tool for the polymer structure visualization. Briefly, AFM images were obtained on an Agilent 5500 AFM/SPM microscope (Agilent Technologies, Santa Clara, CA) under acoustic AC mode using Si probes operating at a resonant frequency of 154 kHz. All measurements were carried out at room temperature and acquired images had a resolution of 512 × 512 pixels collected at a speed of 1 line/minute. Freshly cleaved mica surface was used as the substrate for imaging. To acquire images, about 10-50 μl of the prepared sample was pipetted on to the mica surface and allowed to interact with the surface for 1-5 min. Following this, excess solution was dried under a gentle stream of air. Post image processing of AFM images was done using Pico Image software provided with the instrument.

Transmission electron microscopy (TEM)—For TEM, 10 μL of the sample was placed on the Formvar-coated copper grids (Electron Microscopy Science, Hatfield, PA) and negatively stained with 50 μL of 1% (w/v) uranyl acetate for 2-5 min. A Whatman filter paper was used to drain excess liquid, the grids were allowed to air-dry for a minute. Images were acquired using the JEOL 100X transmission electron microscope (Peabody, MA).

In vivo studies

Animals—Female Balb/c mice (6-8 weeks) and nude female mice (6-8 weeks) were procured from Charles River Laboratory (CRL, Wilmington, MA). Animals were housed in sterile cages with *ad libitum* access to sterile food and water on a 12:12 light/dark cycle. All experiments were approved by the Northeastern University-Institutional Animal Care and Use Committee (NUIACUC).

Biodistribution study—Female Balb/c mice were inoculated with 4T1 tumors by resuspending 2×10^5 cultured cells into sterile phosphate buffer saline (100 μL) injected subcutaneously into the right hind flank of anesthetized animals. Once tumors had reached a palpable volume of at least 100 mm^3, mice were randomly assigned to one of four treatment groups (naked siRNA, PEI/siRNA, DOPE-PEI/siRNA and DOPE-PEI/PEG/siRNA all complexed with FL-siRNA at N/P 16 in a manner similar to that described previously under sample preparation. The siRNA dose was 1.2 mg/kg (40μg/animal). All the formulations were prepared in nuclease-free, filtered HEPES buffered glucose (HBG), pH 7.4. The mice were sacrificed 4h after treatment. Organs were harvested and t h e blood w a s collected via the cardiac puncture method. The organs were homogenized in cold HBG, centrifuged (15,000 g for 20 min at 4°C) to obtain a clear supernatant, and the serum was collected from the derived blood. The organ homogenates and serum were transferred to a 96 well plate and the fluorescence from the samples was read in a fluorescence plate reader at λ_{ex} 485/20, λ_{em}

528/20. Fluorescence values were converted into percent injected dose/gm tissue (% ID/g tissue) or (% ID/ml of serum) from standard curves plotted separately for every tissue type, obtained by spiking varying amounts of FL-siRNA in the organ supernatants or serum [64, 65]. The percentage of recovery was approximately 80% for all the organs except for the tumor (56%).

Comparative evaluation of MDR1 levels in orthotopic vs subcutaneous MCF7/ADR tumor xenografts—MCF7 wild type (MCF7/S) or MCF7/ADR cells were inoculated in three different groups (n=3) of nude female mice. For each mouse, 5×10^6 cells in complete DMEM media were resuspended into Matrigel® from BD Biosciences (San Jose, CA) to yield a total volume of 100 μl.

For the first group, this mixture was injected into the mammary fat pad of isoflurane anesthetized animals after which they were left to rest until tumors reached a palpable volume. For the second group, silastic tubing was cut into 1cm × 1cm lengths and one end was plugged with a silicone rubber sealant. Estradiol was mixed with cholesterol at a weight ratio of 1:100 and ground in a mortar and pestle. About 2.3 mg of the mixture was added into each tube, followed by sealing as before [33]. The filled implants were wiped clean, sterilized with UV radiation overnight and stored sterile before use. These were then implanted surgically at the back of the neck of the three nude female mice. A couple of days were allowed for the mice to recover and 5×10^6 MCF7/ADR cells, resuspended in Matrigel®, were injected orthotopically into the mammary fat pad of these mice. For the third group, 5×10^6 MCF7/ADR cells were resuspended in Matrigel® to yield a total volume of 100 μl and this cell suspension was injected subcutaneously near the right flank region of the nude female mice.

Five weeks post injection, RT-PCR was performed on the excised tumors from three groups. An orthotopic tumor, grown in nude female mice, from MCF7/S cells, in the presence of β-estradiol was also used for MDR1 gene expression evaluation. Briefly, this tumor was developed by injecting 2 million MCF7/S cells subcutaneously over the right flank of nude female mice surgically implanted with an estradiol pellet (as described previously) over the back of the neck of the mouse.

Therapeutic efficacy study—Nude female mice were injected subcutaneously near the right flank with 5×10^6 cells MCF7/ADR cells/mouse, resuspended in Matrigel® for a total volume of 100 μl. Treatments were started when the tumors reached a volume of 60 mm^3, which was designated as day 0 and the mice were randomly assigned to five different treatment groups (n=5). Each tumor bearing animal received intravenous injection of the prepared formulations (see treatment formulations listed below). The dose of the therapeutic MDR1 siRNA (siMDR1) and Dox.HCl (Dox) employed were 1.2 mg/kg and 2 mg/kg, respectively. The dosing regimen was one naked siRNA or formulation-containing siRNA injection followed by one Dox injection after 48 h at one such regimen per week for five weeks. The treatment used were (1) Sterile HEPES buffered glucose 5% (HBG); (2) Free siMDR1 + Dox; (3) DOPE-PEI/siMDR1 + Dox; (4) DOPE-PEI/scramble siRNA) + Dox and (5) DOPE-PEI/PEG/siMDR1 + Dox.

Animals were periodically monitored for body weight and tumor volume. The tumor volume was measured with a digital caliper and calculated as ½ $(S)^2(L)$, where S is the smaller dimension and L is the larger dimension of the tumor. Also mean relative tumor volume (RTVm) was measured for each group and defined as: RTV= Vn/Vo, where Vn was the volume in mm^3 on day 'n' and Vo at the start of treatment. At the end of 40 days post-treatment, blood was collected via the cardiac puncture method from all the mice. Serum was obtained by centrifugation of the freshly collected blood samples at 2,000 g for 30 min at 4 °C and stored at −80°C for further analysis. The tumors were excised after the animals were sacrificed. The volume and the weight of the excised tumors were recorded and then flash frozen in liquid nitrogen for further analysis.

Toxicity Evaluation in Mice—The percent change in body weight was calculated at the end of the study and reported as an indication of general toxicity. The serum aspartate amino transferase (AST) and alanine amino transferase (ALT) levels were also measured and reported as a more reliable indication of repeated dosing toxicity. AST and ALT values were measured by a colorimetric assay method using the manufacturer's standard kinetic assay protocol.

RT-PCR for evaluation of MDR1 levels in excised tumors—Tumors were excised post-mortem and RT-PCR was performed as follows: Isolated tumors were homogenized and processed for RNA isolation using the RNAeasy kit. Isolated RNA was further treated with DNAse. RNA was quantified and quality was evaluated using a ND-1000 NanoDrop spectrophotometer from ThermoScientific® (Wilmington, DE). Primer sequences for both the MDR1 (gene of interest) and GAPDH (housekeeping gene) were adopted from reference [57]. The primers were evaluated using the Invitrogen OligoPerfect™ for GC content, annealing temperature and primer-dimer formation. GAPDH was used as an appropriate internal loading control for RT-PCR. cDNA synthesis and subsequent PCR amplification was performed using the first strand cDNA synthesis kit. Finally, RT-PCR was performed on the tumor samples for each treatment using the LightCycler® 480 RT-PCR machine from Roche™ (IN, USA). The assay was run in 96-well optical reaction plates. Data was normalized to GAPDH and relative quantification method was used for data analysis.

Flow cytometry to evaluate P-gp (MDR1) down-regulation—Excised tumors were minced using two surgical blades with vortexing in a 50ml tube containing 1ml cold PBS. Cell suspension was collected (500μl × 2 aliquots). Aliquot 1 was incubated with FITC-labeled anti P-gp antibody, and aliquot 2 was incubated with non-specific IgG1-FITC antibody (same antibody concentrations for each sample) for 1 hour on ice. Samples were suitably diluted with sheath liquid, flow cytometry was performed and mean fluorescence intensity (MFI) was corrected for fluorescence due to non-specific binding.

Therapeutic efficacy study with co-therapy of siRNA/drug—A second therapeutic efficacy experiment was also conducted which included a group of nude female mice that were simultaneously injected with DOPE-PEI/siRNA and Dox. We performed the same evaluations that were carried out in the previous therapeutic efficacy study, viz. RTVm,

body weight monitoring, AST/ALT, MDR1 and P-gp expression. The treatments used were (1) Free siMDR1 + Dox; (2) DOPE-PEI/siMDR1 + Dox (sequential); and (3) DOPE-PEI/siMDR1 + Dox (simultaneous).

Statistical analysis—Results are presented as mean ± SD. Statistical analysis was performed using GraphPad Prism 5.04 (GraphPad Software Inc. CA, USA). One way ANOVA-Bonferroni's multiple comparisons test or Two way ANOVA were used for data analysis. A P-value less than 0.05 was considered to be statistically significant.

ACKNOWLEDGEMENT

This study was supported with the NIH grant U54CA151881 to VT.

REFERENCES

1. Perez E. Impact, mechanisms, and novel chemotherapy strategies for overcoming resistance to anthracyclines and taxanes in metastatic breast cancer. Breast Cancer Res Treat. 2009; 114:195–201. [PubMed: 18443902]
2. Wind NS, Holen I. Multidrug Resistance in Breast Cancer: From In Vitro Models to Clinical Studies. Int J of Breast Cancer. 2011; 2011:1–12.
3. Riordan JR, Deuchars K, Kartner N, Alon N, Trent J, Ling V. Amplification of P-glycoprotein genes in multidrug-resistant mammalian cell lines. Nature. 1985; 316:817–819. [PubMed: 2863759]
4. Mechetner E, Kyshtoobayeva A, Zonis S, Kim H, Stroup R, Garcia R, et al. Levels of multidrug resistance (MDR1) P-glycoprotein expression by human breast cancer correlate with in vitro resistance to taxol and doxorubicin. Clin Cancer Res. 1998; 4:389–398. [PubMed: 9516927]
5. Hilary Thomas HMC. Overcoming Multidrug Resistance in Cancer:An Update on the Clinical Strategy of Inhibiting P-Glycoprotein. Cancer Control. 2003; 10:150–165.
6. Saraswathy M, Gong S. Different strategies to overcome multidrug resistance in cancer. Biotechnol Adv. 2013; 31:1397–1407. [PubMed: 23800690]
7. Coley, HM. Overcoming Multidrug Resistance in Cancer: Clinical Studies of P-Glycoprotein Inhibitors. In: Zhou, J., editor. Multi-Drug Resistance in Cancer. Humana Press; New Jersey: 2010. p. 341-358.
8. Ozben T. Mechanisms and strategies to overcome multiple drug resistance in cancer. FEBS Lett. 2006; 580:2903–2909. [PubMed: 16497299]
9. Binkhathlan Z, Lavasanifar A. P-glycoprotein Inhibition as a Therapeutic Approach for Overcoming Multidrug Resistance in Cancer: Current Status and Future Perspectives. Curr Cancer Drug Tar. 2013; 13:326–346.
10. Lee, C. Reversing Agents for ATP-Binding Cassette Drug Transporters. In: Zhou, J., editor. Multi-Drug Resistance in Cancer. Humana Press; New Jersey: 2010. p. 325-340.
11. Abbasi M, Lavasanifar A, Uludă H. Recent attempts at RNAi-mediated P-glycoprotein downregulation for reversal of multidrug resistance in cancer. Med Res Rev. 2013; 33:33–53. [PubMed: 21523793]
12. Stege, A.; Krühn, A.; Lage, H. Overcoming Multidrug Resistance by RNA Interference. In: Zhou, J., editor. Multi-Drug Resistance in Cancer. Humana Press; 2010. p. 447-465.
13. Kruehn AWA, Fruehauf J, Lage H. Delivery of short hairpin RNAs by transkingdom RNA interference modulates the classical ABCB1-mediated multidrug-resistant phenotype of cancer cells. Cell Cycle. 2009; 8:3349–3354. [PubMed: 19770582]
14. Xia Z, Zhu Z, Zhang L, Royal C, Liu Z, Chen Q, et al. Specific reversal of MDR1/P-gp-dependent multidrug resistance by RNA interference in colon cancer cells. Oncol Rep. 2008; 20:1433–9. [PubMed: 19020725]
15. Aagaard L, Rossi JJ. RNAi therapeutics: principles, prospects and challenges. Adv Drug Deliver Rev. 2007; 59:75–86.

16. Won YY, Sharma R, Konieczny SF. Missing pieces in understanding the intracellular trafficking of polycation/DNA complexes. J Control Release. 2009; 139:88–93. [PubMed: 19580830]
17. Benjaminsen RV, Mattebjerg MA, Henriksen JR, Moghimi SM, Andresen TL. The possible "proton sponge" effect of polyethylenimine (PEI) does not include change in lysosomal pH. Mol Ther. 2013; 21:149–57. [PubMed: 23032976]
18. Zhong D, Jiao Y, Zhang Y, Zhang W, Li N, Zuo Q, et al. Effects of the gene carrier polyethyleneimines on structure and function of blood components. Biomaterials. 2013; 34:294–305. [PubMed: 23069714]
19. Kunath K, von Harpe A, Fischer D, Petersen H, Bickel U, Voigt K, et al. Low-molecular-weight polyethylenimine as a non-viral vector for DNA delivery: comparison of physicochemical properties, transfection efficiency and in vivo distribution with high-molecular-weight polyethylenimine. J Control Release. 2003; 89:113–25. [PubMed: 12695067]
20. Godbey WT, Wu KK, Mikos AG. Size matters: Molecular weight affects the efficiency of poly(ethylenimine) as a gene delivery vehicle. J Biomed Mater Res. 1999; 45:268–275. [PubMed: 10397985]
21. Navarro G, Sawant R, Essex S, Tros de Ilarduya C, Torchilin V. Phospholipid–polyethylenimine conjugate-based micelle-like nanoparticles for siRNA delivery. Drug Del and Transl Res. 2011; 1:25–33.
22. Navarro G, Sawant RR, Biswas S, Essex S, Tros de Ilarduya C, Torchilin VP. P-glycoprotein silencing with siRNA delivered by DOPE-modified PEI overcomes doxorubicin resistance in breast cancer cells. Nanomedicine (Lond). 2012; 7:65–78. [PubMed: 22191778]
23. Torchilin V. Tumor delivery of macromolecular drugs based on the EPR effect. Adv Drug Del Rev. 2011; 63:131–135.
24. Maeda H. The enhanced permeability and retention (EPR) effect in tumor vasculature: the key role of tumor-selective macromolecular drug targeting. Adv Enzyme Regul. 2001; 41:189–207. [PubMed: 11384745]
25. Maeda H, Bharate GY, Daruwalla J. Polymeric drugs for efficient tumor-targeted drug delivery based on EPR-effect. Eur J Pharm Biophar. 2009; 71:409–419.
26. Sawant RR, Sriraman SK, Navarro G, Biswas S, Dalvi RA, Torchilin VP. Polyethyleneiminelipid conjugate-based pH-sensitive micellar carrier for gene delivery. Biomaterials. 2012; 33:3942–3951. [PubMed: 22365809]
27. Wang J, Mongayt D, Torchilin VP. Polymeric micelles for delivery of poorly soluble drugs: preparation and anticancer activity in vitro of paclitaxel incorporated into mixed micelles based on poly (ethylene glycol)-lipid conjugate and positively charged lipids. J Drug Target. 2005; 13:73–80. [PubMed: 15848957]
28. Pulaski, BA.; Ostrand-Rosenberg, S. Mouse 4T1 Breast Tumor Model. In: Coligan, JE.; Bierer, BE.; Margulies, DH.; Shevach, EM.; Strober, W., editors. Current Protocols in Immunology. John Wiley and Sons, Inc; New York: 2001.
29. Ciardiello F, Caputo R, Borriello G, Del Bufalo D, Biroccio A, Zupi G, et al. ZD1839 (IRESSA), an EGFR-selective tyrosine kinase inhibitor, enhances taxane activity in bcl-2 overexpressing, multidrug-resistant MCF-7 ADR human breast cancer cells. Int J Cancer. 2002; 98:463–469. [PubMed: 11920601]
30. Dubois V, Dasnois L, Lebtahi K, Collot F, Heylen N, Havaux N, et al. CPI-0004Na, a New Extracellularly Tumor-Activated Prodrug of Doxorubicin In Vivo Toxicity, Activity, and Tissue Distribution Confirm Tumor Cell Selectivity. Cancer Res. 2002; 62:2327–2331. [PubMed: 11956091]
31. Fu L, Zhang Y, Liang Y, Yang X, Pan Q. The multidrug resistance of tumour cells was reversed by tetrandrine *in vitro* and in xenografts derived from human breast adenocarcinoma MCF-7/adr cells. Eur J Cancer. 2002; 38:418–426. [PubMed: 11818209]
32. Lu H-L, Syu W-J, Nishiyama N, Kataoka K, Lai P-S. Dendrimer phthalocyanine-encapsulated polymeric micelle-mediated photochemical internalization extends the efficacy of photodynamic therapy and overcomes drug-resistance in vivo. J Control Release. 2011; 155:458–464. [PubMed: 21689700]

33. van Vlerken LE, Duan Z, Little SR, Seiden MV, Amiji MM. Augmentation of therapeutic efficacy in drug-resistant tumor models using ceramide coadministration in temporal-controlled polymer-blend nanoparticle delivery systems. AAPS J. 2010; 12:171–180. [PubMed: 20143195]
34. Lee ES, Na K, Bae YH. Doxorubicin loaded pH-sensitive polymeric micelles for reversal of resistant MCF-7 tumor. J Control Release. 2005; 103(2):405–18. [PubMed: 15763623]
35. Gao Y, Chen L, Zhang Z, Chen Y, Li Y. Reversal of multidrug resistance by reduction-sensitive linear cationic click polymer/iMDR1-pDNA complex nanoparticles. Biomaterials. 2011; 32(6): 1738–47. [PubMed: 21112086]
36. Jiang J, Yang S, Wang J, Yang L, Xu Z, Yang T, et al. Sequential treatment of drug-resistant tumors with RGD-modified liposomes containing siRNA or doxorubicin. Eur J Pharm Biopharm. 2010; 76:170–178. [PubMed: 20600887]
37. Boone L, Meyer D, Cusick P, Ennulat D, Bolliger AP, Everds N, et al. Selection and interpretation of clinical pathology indicators of hepatic injury in preclinical studies. Vet Clin Path. 2005; 34:182–188. [PubMed: 16134065]
38. Kratz F, Warnecke A. Finding the optimal balance: Challenges of improving conventional cancer chemotherapy using suitable combinations with nano-sized drug delivery systems. J Control Release. 2012; 164:221–235. [PubMed: 22705248]
39. Lu D, Wientjes MG, Lu Z, Au JL-S. Tumor Priming Enhances Delivery and Efficacy of Nanomedicines. J Pharmacol Exp Ther. 2007; 322:80–88. [PubMed: 17420296]
40. MacDiarmid JA, Amaro-Mugridge NB, Madrid-Weiss J, Sedliarou I, Wetzel S, Kochar K, et al. Sequential treatment of drug-resistant tumors with targeted minicells containing siRNA or a cytotoxic drug. Nature Biotechnol. 2009; 27:643–651. [PubMed: 19561595]
41. Meng H, Mai WX, Zhang H, Xue M, Xia T, Lin S, et al. Codelivery of an Optimal Drug/siRNA Combination Using Mesoporous Silica Nanoparticles To Overcome Drug Resistance in Breast Cancer in Vitro and in Vivo. ACS Nano. 2013; 7:994–1005. [PubMed: 23289892]
42. Yadav S, van Vlerken LE, Little SR, Amiji MM. Evaluations of combination MDR-1 gene silencing and paclitaxel administration in biodegradable polymeric nanoparticle formulations to overcome multidrug resistance in cancer cells. Cancer Chemoth and Pharm. 2009; 63:711–722.
43. Gebhart CL, Sriadibhatla S, Vinogradov S, Lemieux P, Alakhov V, Kabanov AV. Design and formulation of polyplexes based on pluronic-polyethyleneimine conjugates for gene transfer. Bioconjugate Chem. 2002; 13:937–44.
44. Shen J, Yin Q, Chen L, Zhang Z, Li Y. Co-delivery of paclitaxel and survivin shRNA by pluronic P85-PEI/TPGS complex nanoparticles to overcome drug resistance in lung cancer. Biomaterials. 2012; 33:8613–24. [PubMed: 22910221]
45. Chen Y, Zhu X, Zhang X, Liu B, Huang L. Nanoparticles modified with tumor-targeting scFv deliver siRNA and miRNA for cancer therapy. Mol Ther. 2010; 18(9):1650–6. [PubMed: 20606648]
46. Kim SH, Jeong JH, Lee SH, Kim SW, Park TG. Local and systemic delivery of VEGF siRNA using polyelectrolyte complex micelles for effective treatment of cancer. J Control Release. 2008; 129(2):107–16. [PubMed: 18486981]
47. Malek A, Merkel O, Fink L, Czubayko F, Kissel T, Aigner A. In vivo pharmacokinetics, tissue distribution and underlying mechanisms of various PEI(-PEG)/siRNA complexes. Toxicol Appl Pharm. 2009; 236:97–108.
48. Merkel OM, Librizzi D, Pfestroff A, Schurrat T, Buyens K, Sanders NN, et al. Stability of siRNA polyplexes from poly(ethylenimine) and poly(ethylenimine)-g-poly(ethylene glycol) under in vivo conditions: effects on pharmacokinetics and biodistribution measured by Fluorescence Fluctuation Spectroscopy and Single Photon Emission Computed Tomography (SPECT) imaging. J Control Release. 2009; 138:148–59. [PubMed: 19463870]
49. Dykxhoorn DM, Palliser D, Lieberman J. The silent treatment: siRNAs as small molecule drugs. Gene Ther. 2006; 13:541–552. [PubMed: 16397510]
50. Zuckerman JE, Choi CH, Han H, Davis ME. Polycation-siRNA nanoparticles can disassemble at the kidney glomerular basement membrane. Proc Natl Acad Sci USA. 2012; 109:3137–42. [PubMed: 22315430]

51. Appleyard MV, O'Neill MA, Murray KE, Paulin FE, Bray SE, Kernohan NM, et al. Seliciclib (CYC202, R-roscovitine) enhances the antitumor effect of doxorubicin in vivo in a breast cancer xenograft model. Int J Cancer. 2009; 124:465–72. [PubMed: 19003963]
52. Grosse PY, Bressolle F, Pinguet F. Antiproliferative effect of methyl-beta-cyclodextrin in vitro and in human tumour xenografted athymic nude mice. Br J Cancer. 1998; 78:1165–9. [PubMed: 9820174]
53. Li Q, Lv S, Tang Z, Liu M, Zhang D, Yang Y, et al. A co-delivery system based on paclitaxel grafted mPEG-b-PLG loaded with doxorubicin: Preparation, in vitro and in vivo evaluation. Int J Pharm. 2014; 471:412–420. [PubMed: 24905776]
54. Abbasi M, Aliabadi HM, Moase EH, Lavasanifar A, Kaur K, Lai R, et al. siRNA-mediated down-regulation of P-glycoprotein in a Xenograft tumor model in NOD-SCID mice. Pharm Res. 2011; 28:2516–29. [PubMed: 21638135]
55. Yin Q, Shen J, Chen L, Zhang Z, Gu W, Li Y. Overcoming multidrug resistance by co-delivery of Mdr-1 and survivin-targeting RNA with reduction-responsible cationic poly(beta-amino esters). Biomaterials. 2012; 33:6495–506. [PubMed: 22704597]
56. Patil YB, Swaminathan SK, Sadhukha T, Ma L, Panyam J. The use of nanoparticle-mediated targeted gene silencing and drug delivery to overcome tumor drug resistance. Biomaterials. 2010; 31:358–65. [PubMed: 19800114]
57. Xiong X-B, Lavasanifar A. Traceable Multifunctional Micellar Nanocarriers for Cancer-Targeted Co-delivery of MDR-1 siRNA and Doxorubicin. ACS Nano. 2011; 5(6):5202–5213. [PubMed: 21627074]
58. Li J, Wang Y, Zhu Y, Oupicky D. Recent advances in delivery of drug-nucleic acid combinations for cancer treatment. J Control Release. 2013; 172:589–600. [PubMed: 23624358]
59. Mosure KW, Henderson AJ, Klunk LJ, Knipe JO. Disposition of conjugate-bound and free doxorubicin in tumor-bearing mice following administration of a BR96-doxorubicin immunoconjugate (BMS 182248). Cancer Chemoth Pharm. 1997; 40:251–258.
60. Mao S, Neu M, Germershaus O, Merkel O, Sitterberg J, Bakowsky U, et al. Influence of Polyethylene Glycol Chain Length on the Physicochemical and Biological Properties of Poly(ethylene imine)-graft-Poly(ethylene glycol) Block Copolymer/SiRNA Polyplexes. Bioconjugate Chem. 2006; 17:1209–1218.
61. Wu H, Hait WN, Yang J-M. Small Interfering RNA-induced Suppression of MDR1 (PGlycoprotein) Restores Sensitivity to Multidrug-resistant Cancer Cells. Cancer Res. 2003; 63:1515–1519. [PubMed: 12670898]
62. Pakunlu RI, Cook TJ, Minko T. Simultaneous modulation of multidrug resistance and antiapoptotic cellular defense by MDR1 and BCL-2 targeted antisense oligonucleotides enhances the anticancer efficacy of doxorubicin. Pharm Res. 2003; 20:351–9. [PubMed: 12669953]
63. Saad M, Garbuzenko OB, Minko T. Co-delivery of siRNA and an anticancer drug for treatment of multidrug-resistant cancer. Nanomedicine(Lond). 2008; 3:761–776. [PubMed: 19025451]
64. Kim SH, Jeong JH, Lee SH, Kim SW, Park TG. Local and systemic delivery of VEGF siRNA using polyelectrolyte complex micelles for effective treatment of cancer. J Control Release. 2008; 129:107–116. [PubMed: 18486981]
65. Li S-D, Chen Y-C, Hackett MJ, Huang L. Tumor-targeted Delivery of siRNA by Self-assembled Nanoparticles. Mol Ther. 2007; 16:163–169. [PubMed: 17923843]

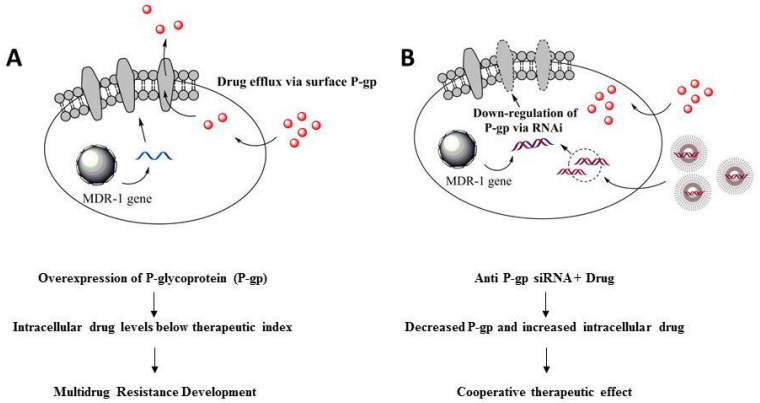

Figure 1.

General scheme of MDR phenomena (A) and anti-P-gp siRNA/drug combination treatment (B). It is well known that there is an active efflux of chemotherapeutic agents like Dox as a result of overexpression of P-gp (encoded by the MDR1 gene) on the tumor cell surface. This leads to a low intracellular drug accumulation (below minimum effective concentration or MEC) and hence, results in failure of chemotherapy. One of the solutions is treatment with therapeutic siRNA that targets the MDR1 gene and thus, brings about the down-regulation of the surface P-gp expression. With conventional chemotherapeutic treatment, drug concentration can reach the therapeutic index window, exert its cytotoxic effects and lead to a successful chemotherapeutic treatment.

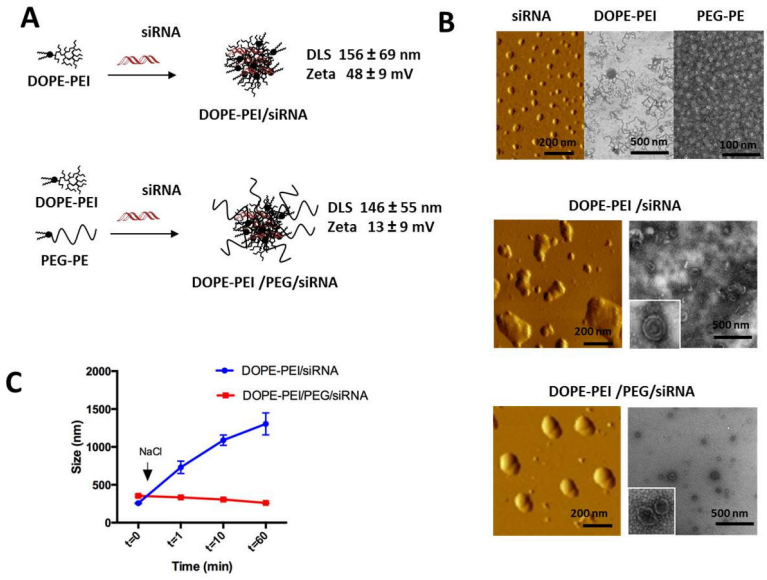

Figure 2.

Biophysical characterization of DOPE-PEI nanocarriers. (A) Schematic illustration of the nanocarriers' assembly with the mean diameter and the zeta potential of the formulations. (B) Detailed structure and morphology of free siRNA, DOPE-PEI and PEG-PE components and assembled nanocarriers by AFM and TEM. (C) Stability of nanocarriers indicated by the change in size after incubation with 150mM NaCl for up to 1h at RT.

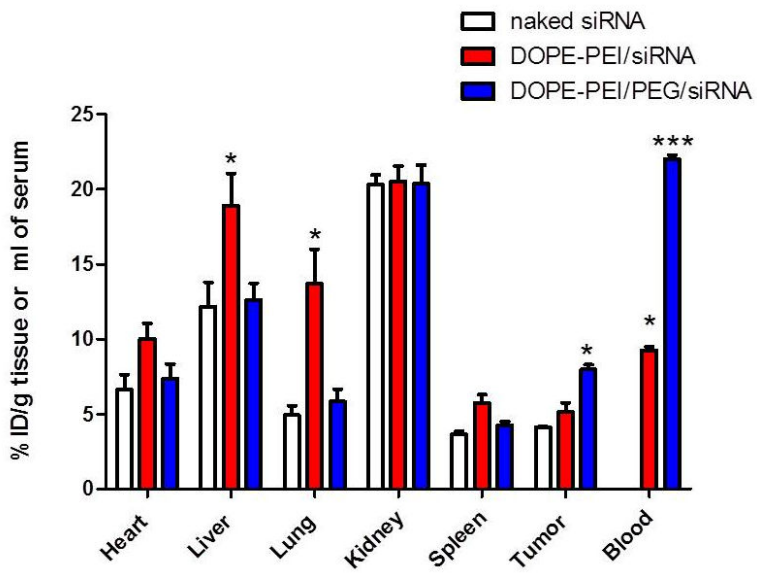

Figure 3.

Biodistribution of fluorescein-labeled siRNA either naked or complexed in formulations 4 h post injection. Results are expressed as mean percentage of injected dose (%ID)g of tissue or mL of serum ± SD (n=5); *P<0.05, ***P<0.001 vs the naked siRNA group.

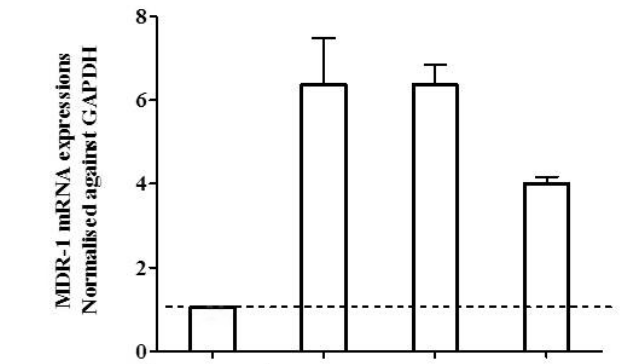

	MCF-7/S	MCF-7/ADR		
Tumor Implantation	orthotopic	orthotopic	orthotopic	s.c.
Hormone Supplementation ?	Yes	Yes	No	No
Tumor size after 5 weeks	250 mm^3	40 mm^3	40 mm^3	100 mm^3

Figure 4.

Levels of mRNA MDR1 in orthotopic and s.c. tumors measured 5 weeks after tumor implantation by qRT-PCR.

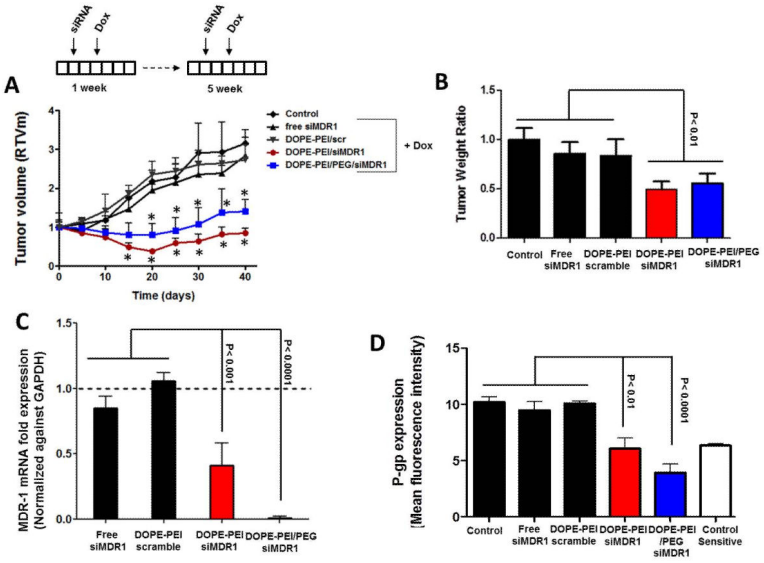

Figure 5.

Anti-tumor effect of siRNA targeting P-glycoprotein (siMDR1) in DOPE-PEI nanocarriers and Dox using nude mice bearing MCF-7/ADR tumors. Mice were intravenously injected once per week with BHG, free siRNA or different DOPE-PEI formulations followed by Dox injection (after 48 h) for 5 weeks. (A) Relative tumor volume (RTV) and (B) tumor weight ratio for the different treatments. Results are plotted as mean ± SD. (n=5). (C) Levels of mRNA MDR1 and (D) P-glycoprotein at the final time-point. Results are plotted as mean ± SD (n=5, C and D performed in duplicates and triplicates, respectively). *P < 0.001 vs BHG, free siMDR1 and DOPE-PEI/scramble siRNA.

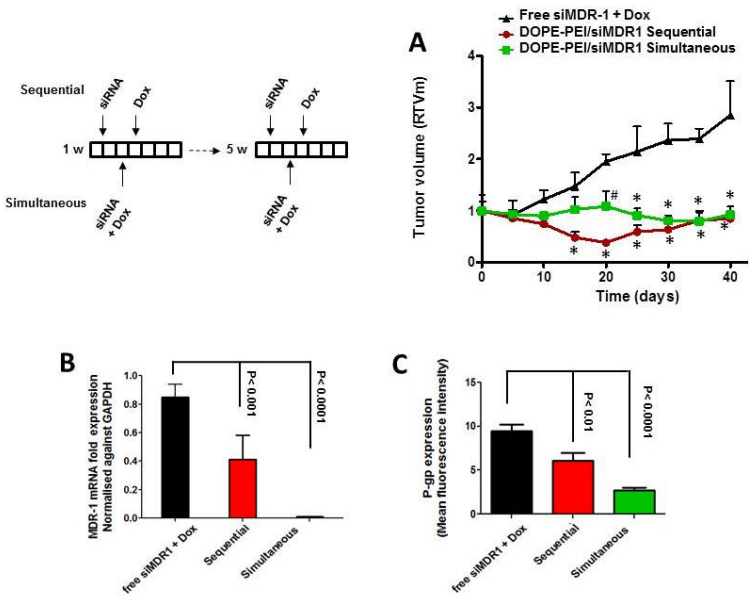

Figure 6.

Anti-tumor effect of siRNA targeting P-glycoprotein (siMDR1) in DOPE-PEI nanocarriers with Dox sequentially or simultaneously administered in nude mice bearing MCF-7/ADR tumors. (A) Relative tumor volume (RTV) for the different treatments. (B) Levels of mRNA MDR1 and (C) P-glycoprotein at final time-point. Results are plotted as mean ± SD n=5, B and C performed in duplicates and triplicates, respectively). *P < 0.001 # P < 0.01 vs free siMDR1 + Dox

Table 1

Treatment	AST (IU/L)	ALT (IU/L)	% change in body weight (from day 0)
Control	11.2 ± 0.1	15.0 ± 0.1	1%
Free siMDR1	14.1± 0.3	16.9 ± 0.1	1%
DOPE-PEI/scramble	12.9 ± 0.1	16.2 ± 0.1	1%
DOPE-PEI/siMDR1	13.2 ± 0.2	19.4 ± 0.3	7%
DOPE-PEI/PEG/siMDR1	20.3 ± 0.5	21.2 ± 0.3	0.30%

Table 2

Treatment	AST (IU/L)	ALT (IU/L)	% change in body weight (from day 0)
Free siMDR1+Dox	14.0 ± 0.3	17.0 ± 0.1	1%
Sequential	13.2 ± 0.2	19.4 ± 0.3	7.20%
Simultaneous	11.0 ± 0.5	17.0 ± 0.2	0.10%